

ANALYSIS OF THE PROCESS OF AMPLIFICATION IN A SINGLE PASS FEL OF HIGH ORDER HARMONICS GENERATED IN A GAS JET

L. Giannessi, M. Quattromini, ENEA C.R. Frascati, Frascati (Roma) Italy

P. Musumeci, INFN Sez. Roma I, Roma, Italy

G. Sansone, S. Stagira, M. Nisoli, S. De Silvestri, Politecnico di Milano, Milano, Italy.

Abstract

We have studied the amplification of high harmonics generated by a short infrared pulse in a gas jet, injected in a free electron laser amplifier. The high-order harmonic spectra have been simulated using a 3D non-adiabatic model that includes both the single atom response and the effect of the propagation of the XUV field inside the gas jet. The response of a single atom to the IR field is calculated in the framework of the Strong Field Approximation (SFA); The nonlinear polarization associated to this process is evaluated as the acceleration of the nonlinear dipole moment. This term is used as source term in the propagation of the harmonic field inside the gas jet. The propagation effect are extremely relevant for the temporal structure of the XUV field as the coherent interference of the dipole emission of the different atoms leads to the selection of only one XUV pulse for each semi-cycle of the driving IR field. The amplification in the free electron laser has been simulated with GENESIS 1.3. The effects of filtering the seed spectrum have been analyzed and the coherence properties of the light are considered.

INTRODUCTION

The FEL amplification in the SASE regime [1] leads to a longitudinal pulse shape and amplitude governed by the stochastic properties of the electron beam shot noise. The result is a reduced longitudinal coherence and intrinsic pulse to pulse energy fluctuations [2]. A single pass FEL, seeded with an external source, shows a number of advantages with respect to SASE, as the control over the pulse shape better coherence properties which are determined by the seed [3,4]. Intense seed sources are available in the visible and UV region of the spectrum based on reliable solid state laser technology. The FEL operating range may be extended to shorter wavelengths with cascaded schemes, i.e. taking advantage of the harmonic generation process in the FEL dynamics[5]. On the other hand high harmonic multiplication factors in a multi-stage cascade FEL are limited by the energy spread induced in each stage by the FEL process and these configurations are affected by stability issues associated to the fluctuation of one or more of the large number of parameters defining the configuration [6,7]. An alternative to a multi-stage cascade with a high harmonic multiplication factor is that of seeding the FEL amplifier directly at short wavelengths with the high order harmonics of an intense Ti:Sa laser pulse generated in a

Gas Jet [8]. Such a possibility is considered in the scheme of several proposed facilities [9,10,11] and experiments are planned in the next future [12,13]. The high frequency field produced in the interaction with the gas jet has some very peculiar features. The pulse has a spiky structure, with attosecond pulses separated by half of the drive laser wavelength [14]. The spectrum contains the odd harmonics of the Ti:Sa drive laser and extends to short wavelengths with a cut-off depending on the nature of the gas used. The energy per pulse drops rapidly at the shortest wavelengths, where the combination of this seed source with an FEL amplifier would be more appealing. We are interested in understanding what is the minimum energy required by an FEL amplifier in order to overcome the electron beam shot noise and amplify the harmonic pulse. A threshold intensity was obtained in the case of a seed constituted by a uniform plane wave [15], but it is not clear whether that threshold remains valid when the pulse has the time/spectral structure of the harmonics produced in gas and whether filtering the input seed is required despite of the fact that the FEL has a limited bandwidth proportional to the FEL parameter ρ [1,2]. Start to end simulations of the electron beam dynamics in a single pass FEL have been widely used to understand the dynamics of the coupled system of electrons and fields undergoing the FEL process. In order to answer the previous questions we have implemented a start-to-end simulation from the radiation point of view, starting with the process of harmonic generation in the gas jet and injecting the field distribution in a widespread and reliable FEL simulation code as GENESIS 1.3 [16]. The paper is organized as follows: in the next section we study the generation of the high harmonics field in the gas jet. In the last section we select the field at the target wavelength of 29.6 nm corresponding to the 27th harmonic of the Ti:Sa and we analyse the results of simulations of the seeded FEL amplifier.

HIGH ORDER HARMONICS IN GAS

The high-order harmonic spectra have been simulated using a 3D non-adiabatic model that includes both the single atom response and the effect of the propagation of the XUV field inside the gas jet. The response of a single atom to the IR field is calculated in the framework of the Strong Field Approximation (SFA); in this model the atom is ionized via tunnelling by the IR field and the freed electron is then accelerated by the electric field of the driving pulse. For particular emission instant the

electron can be driven back to the parent ion and can recombine with the ground state emitting the exceeding energy as a photon in the extreme ultraviolet region or soft x ray region. The nonlinear polarizability associated to this process is evaluated as the acceleration of the nonlinear dipole moment:

$$d_{nl}(t) = 2 \operatorname{Re} \left\{ i \int_{-\infty}^t dt' \left[\left(\frac{\pi}{\varepsilon + i(t-t')/2} \right)^{3/2} \exp[-iS_{st}(t,t')] \right] \right. \\ \left. E(t') d^*(p_{st}(t,t') - A(t)) d(p_{st}(t,t') - A(t')) \right\} \quad (1) \\ * \exp \left(- \int_{-\infty}^t w(t') dt' \right)$$

In this equation $E(t)$ and $A(t)$ are respectively the electric field and the vector potential of the driving field; $p_{st}(t,t')$ is the stationary value of the momentum of the freed electron, $S_{st}(t,t')$ is the phase accumulated by the electron wave packet, $d(p)$ and $d^*(p)$ are the dipole matrix element for transitions from the ground state to a continuum state characterized by momentum p . The last term of equation (1) takes into account ground state depletion through the term ionization rate $w(t)$ calculated using the ADK model. The nonlinear dipole moment is used as source term in the propagation of the harmonic field inside the gas jet. The wave propagation equations for the driving and the harmonic field are solved in cylindrical symmetry in the framework of the paraxial approximation. The harmonic power spectrum is obtained integrating over the radial profile the harmonic electric field at the output of the gas jet.

Propagation effects are extremely relevant for a correct simulation of the time structure of the harmonic radiation. Indeed usually the single atom response is characterized by a complex time structure (usually two attosecond pulses for each half optical cycle), whereas the macroscopic time structure of the XUV radiation is characterized by a single attosecond pulse for each semi optical cycle. The origin of this difference is related to the phase matching mechanism operating during the propagation of the XUV field inside the gas jet.

In the process of high order harmonic generation, the electron can follow two different paths in order to recombine with the parent ion. These two paths are usually referred to as the “short” and the “long” path, as they are characterized by different times spent by the electron in the continuum of energy states. For the short path this time is usually less than half the optical period T_0 , while for the long paths this time is typically of the order of the laser period. The coherent superposition of the contributions of these two paths leads to the generation of two attosecond pulses for each half optical cycle of the driving laser field. The coherent interference of the dipole emission of the different atoms inside the gas jet leads to different phase-matching conditions for the two paths. The relative contribution of the two paths

to the harmonic spectra can be enhanced or reduced changing the relative position of the gas jet with respect to the laser focus. The phase-matching condition in the HHG process are indeed determined by the geometric phase of the driving pulse and by the phase accumulated by the electron wave packet during his motion. In particular conditions, gas jet positioned few millimeters after the laser focus, it is possible to efficiently select on the contribution of the short path, leading to the selection of only one XUV pulse for each semi cycle of the driving IR field[17].

In other experimental condition (gas jet before or close to the laser focus), the contribution of the long paths increases and therefore also the time structure of the generated XUV radiation is more complex.

For our simulation we considered a Gaussian beam with a beam waist of $w_0 = 50 \mu\text{m}$ (in the focus), and focused 3mm before a Neon gas jet with a thickness of 1mm. The pulse duration is FWHM=30 fs with a peak intensity in the focus of $1 \times 10^{14} \text{W/cm}^2$. The high frequency portion of the spectrum, in the range 20 nm – 60 nm of the on axis radiation is shown in Fig. 1. The spectrum contains the odd harmonics of the Ti:Sa resonant wavelength (800 nm).

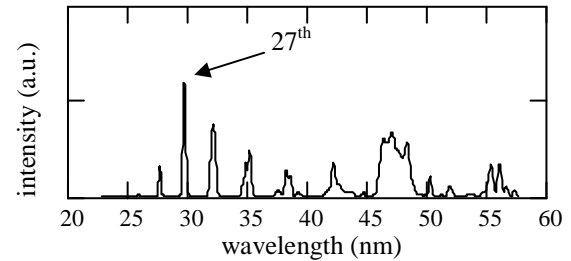


Fig. 1 Short wavelength spectrum of the HHG seed field.

The slowly varying envelope approximation (SVEA) has not been used in the model, but the FEL dynamics studied with GENESIS 1.3 rely on this approximation.

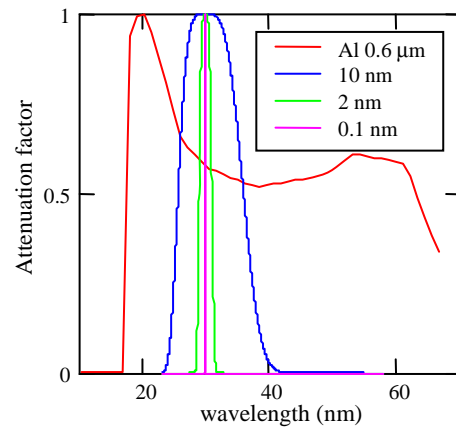


Fig. 2 Attenuation factor as a function of the wavelength of the different filters used in the simulations. The red line correspond to 600 nm layer of Aluminium.

For this reason we have to limit the bandwidth of the input signal by filtering the seed field and define the

slowly varying field as $\tilde{E}(z) = E(z)\exp(-ik_0z)$ where k_0 is the FEL central resonant wave vector. In our example we consider filtering with different bandwidth as shown in Fig.2 centered at the resonant wavelength $\lambda_0 = 2\pi/k_0 = 29.66\text{nm}$ corresponding to the 27th harmonic of the Ti:Sa (Fig.1).

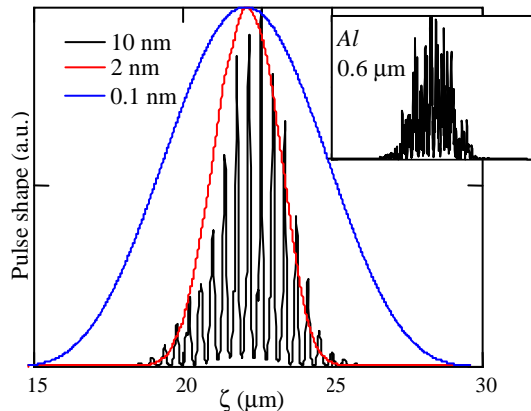


Fig. 3 Longitudinal pulse profile of the input seed after filtering. The plot in the upper right corner is the pulse shape filtered only with the Al broadband filter.

The effect of filtering on the seed temporal profile is shown in Fig. 3. The 10nm bandwidth is wide enough to preserve the attosecond structure of the input field. At 2nm the bandwidth preserves the pulse envelope, but overrides the fine structure. The 0.1nm filter induces an increase of the pulse length.

THE FEL SIMULATION

The FEL configuration considered is based on the parameters shown in Tab. 1. The FEL parameter is $\rho \sim 10^{-3}$ and an estimate of the seed intensity necessary to override the e-beam shot noise as calculated in ref.[15] is about $I_0 \approx 0.3\text{MW/cm}^2$.

Table 1: FEL configuration parameters

Beam Energy (GeV)	1
Peak current (A)	1000
Energy Spread (%)	0.06
Emittance (mm-mrad)	1
Average β_T (m)	6
Undulator period (cm)	4.2
K (peak)	2.97
Periods per section	58
Sections	7

The field spot size and divergence have been matched to the e-beam optical functions by propagation through a drift+lens+drift optical system. The field phase and amplitude at the undulator entrance are shown in Fig.4.

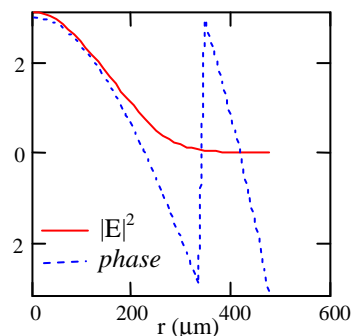


Fig. 4 Transverse field at the undulator entrance averaged over z .

The radiation power as a function of the longitudinal coordinate in the electron beam frame (horizontal) and position along the undulator at the coordinate z (vertical) is shown in Fig.5. The power is normalized at each z . The plots have been obtained by different filtering of the seed. The input seed energies, 2.5nJ@10nm, 1nJ@2nm and 0.5nJ@0.1nm have been chosen in order the energy in a bandwidth 2ρ to be roughly the same (0.5nJ) in the three cases.

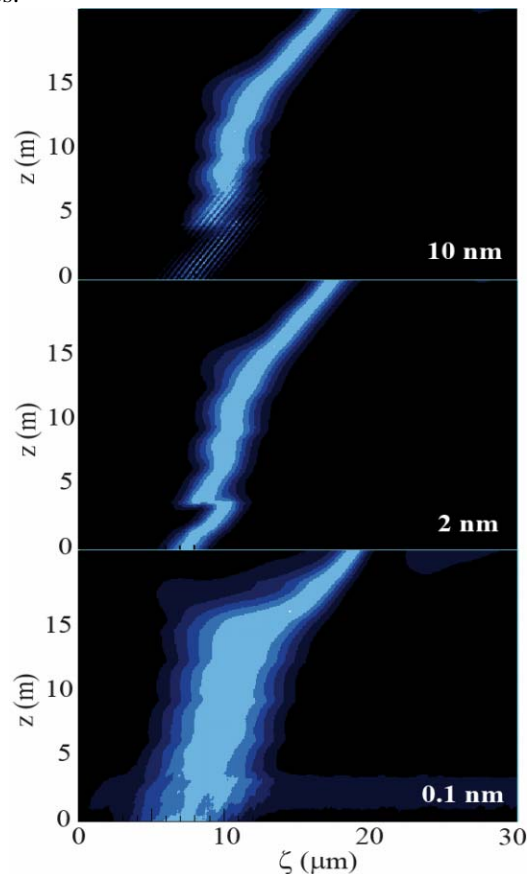


Fig. 5 Normalized longitudinal profile of the radiation power as a function of the longitudinal coordinate in the electron beam frame as it evolves along the undulator with coordinate z . The seed has been filtered at different bandwidths.

The fine structure present in the 10nm case is wiped out by the finite bandwidth of the FEL. The different filtering

affects the pulse shape only before saturation, which occurs at about 15m in all cases. Thereafter the pulse enters the superradiant regime where the pulse length is related to the peak power and is the same in all cases. The

The input seed intensity is $15\text{MW}/\text{cm}^2@10\text{nm}$, $8.5\text{MW}/\text{cm}^2@2\text{nm}$, and $4\text{MW}/\text{cm}^2@0.1\text{nm}$ averaged over z , always much larger than I_0 . In Fig. 6, the simulation corresponding to 0.1nm has been repeated with input energies 0.05nJ and 0.01nJ, corresponding to intensities slightly above and below the threshold I_0 respectively. In both cases SASE is clearly visible at the beginning. In the latter case a structure in the pulse with loss of longitudinal coherence is present and SASE spikes compete with the seeded signal until saturation.

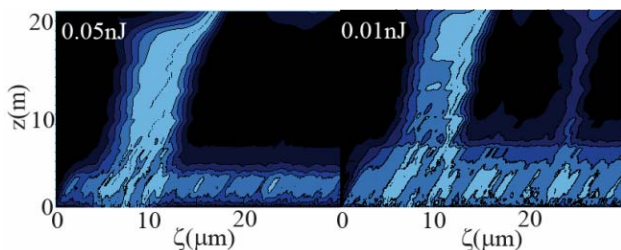


Fig. 6 Same as in Fig.5, case with 0.1nm BW above (left) and below (right) the threshold I_0 .

The input energy levels considered are however very conservative. In fact recent results [18] have demonstrated the feasibility of pulses with energies up to several hundreds nanojoules at the considered photon wavelength. In Fig. 7 the power vs. ζ and z as in Figs. 5 and 6 (left) and the spectrum (right) are shown for the $100\text{nJ}@10\text{nm}$ case. Saturation is reached after only 8m. The splitting of the spectrum typical of the superradiant regime is clearly visible at the end of the undulator.

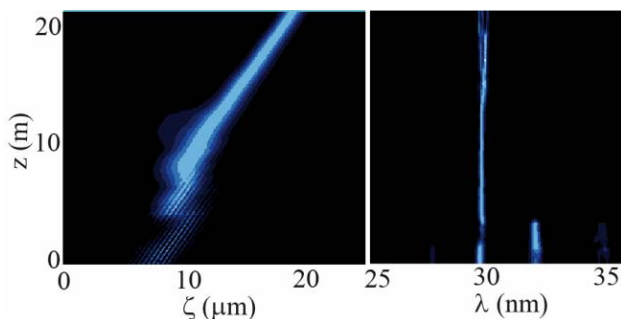


Fig. 7 Normalized longitudinal profile of the radiation power as a function of the longitudinal coordinate in the electron beam frame as it evolves along the undulator with coordinate z (upper plot). Corresponding wavelength spectrum as a function of z .

CONCLUSIONS

In this paper we have presented an analysis of the dynamics of a FEL seeded with the high order harmonics generated in gas. The minimum seed energy has been estimated in a specific FEL configuration with the resonance at the 27th harmonic of the Ti:Sa drive laser.

The results are in reasonable agreement with the threshold estimation in [15]. Currently available sources in the XUV appears to be sufficiently intense to implement such a scheme. The analysis in the frequency domain, suggests that filtering the seed it is not necessary unless a line-width smaller than the natural FEL line-width is required.

This work was partially supported by the EU Commission in the Sixth Framework Programme, Contract No. 011935-EUROFEL.

REFERENCES

- [1] R. Bonifacio, C. Pellegrini, and L. M. Narducci, Opt. Commun. 50, 373 (1984)
- [2] E. L. Saldin, E. A. Schneidmiller, M. V. Yurkov, Opt. Commun. 148, 383 (1998)
- [3] L. H. Yu et al., Science 289, 932 (2000)
- [4] L. H. Yu et al. Phys. Rev. Lett. 91, 074801 (2003)
- [5] G. Dattoli et al. Journal of Appl. Phys. 97, 113102 (2005)
- [6] B. Kuske et al. Development of Figures of Merit to Evaluate the Output of FEL HGHG Cascades, MOPPH051, these proceedings
- [7] G. De Ninno et al. Start-to-end Time-Dependent Study of FEL Output Sensitivity to Electron-beam Jitters for the First Stage of the FERMI@Elettra Project, MOPPH058, these proceedings
- [8] D. Garzella *et al.*, Nucl. Instrum. Methods Phys. Res. Sect. A 528, 502 (2004).
- [9] C. Bruni, The Arc En Ciel FEL proposal, MOPPH048, these proceedings
- [10] B. McNeil et al, The Conceptual Design of the 4GLS XUV-FEL, MOPPH012, these proceedings
- [11] C. Vaccarezza et al., Status of the SPARX FEL project , MOPCH028 in procs. of the 2006 EPAC conference (2006).
- [12] G. Lambert, Seeding the FEL of the SCSS Phase I Facility, MOPPH046 these proceedings
- [13] O. Tcherbakoff et al, MOPPH047 these proceedings, see also L. Giannessi, Future seeding experiments at SPARC, MOPPH028 these proceedings
- [14] P. Salieres, M. Lewenstein, Meas. Sci. Technol. 12, 1818 (2001)
- [15] L. Giannessi, Harmonic generation and linewidth narrowing in seeded FEL, in Proc. of the 26th FEL conference, Trieste 2004 JACoW (Joint Accelerator Conference Website) at <http://www.JACoW.org>, p. 37 (2004)
- [16] S. Reiche, Nuclear Instrum. & Meth. A429, 243 (1999)
- [17] P. Salières, B. Carré, L. Le Déroff, F. Grasbon, G. G. Paulus, H. Walther, R. Kopold, W. Becker, D. B. Milosevic, A. Sanpera, M. Lewenstein, Science 292, 902 (2001).
- [18] E.J. Takahashi et al. IEEE J. of Sel. Topics in Q.Elec. 10, 1315 (2004)